Available online at www.sciencedirect.com

ScienceDirect

Procedia Engineering 10 (2011) 3477–3482

Engineering Procedia

ICM11

Analysis of strain rate behavior of an Al 6061 T6 alloy

A. Manes[a]*, L. Peroni[b], M. Scapin[b], M. Giglio[a]

[a]*Politecnico di Milano, Department of Mechanical Engineering*
Via La Masa 1 20156 Milan, Italy
[b]*Politecnico di Torino, Department of Mechanics*
Corso Duca degli Abruzzi 24, 10129 Turin, Italy

Abstract

In order to simulate complex scenario like ballistic impact, correct material calibration is fundamental. The material in the area involved by impact can experience high deformation and damage in a very limited time. As a consequence dynamic tests on the materials are needed in order to calibrate constitutive law able to describe the material behavior in terms of hardening and in particular strain rate. According to the fact that no guidelines are available on testing methods, different types of testing techniques have been used to generate data under dynamic conditions. Several dynamic tests, are carried out on Al 6061 T6 specimens and the experimental data elaborated. The developed procedure is useful to take into account also the thermal phenomena generally affecting high strain-rate tests due to the adiabatic overheating related to the conversion of plastic work. The method presented requires strong effort both from experimental and numerical point of view; anyway it allows to precisely identifying the parameters of a material models. This could provide great advantages when high reliability of the material behavior is necessary.

Keywords: Al 6061 T6; strain rate; thermal softening; Johnson-Cook; inverse method

1. Introduction

Extreme load scenario likes ballistic impact is a present challenge in the design of critical mechanical components. Although experimental testing is fundamental for a reliable approach to structural integrity evaluation, alternative methods as numerical simulations are now an actual option, especially due to the

* Corresponding author. Tel.: +039-02-23998630; fax: +039-02-23998263.
E-mail address: andrea.manes@polimi.it.

 doi:10.1016/j.proeng.2011.04.573

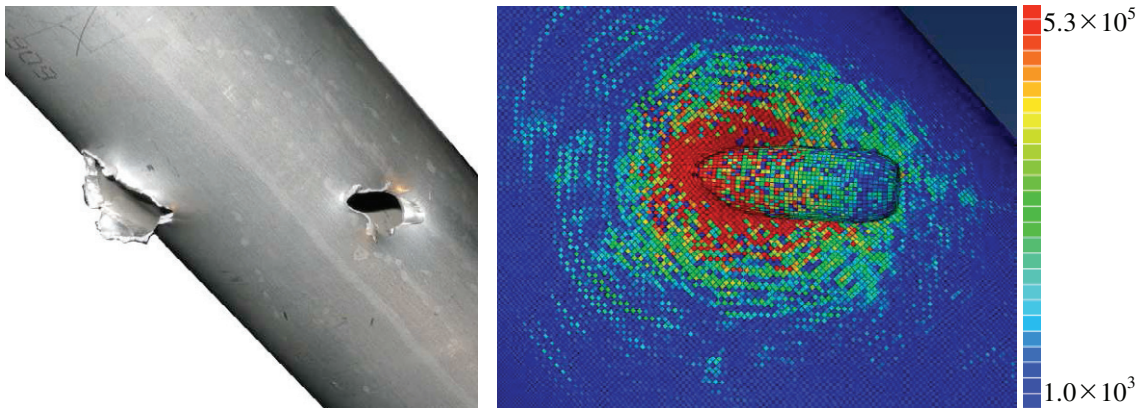

Fig. 1. Real damage consequent to the bullet impact on the helicopter tail rotor transmission (left); numerical result of the strain rate (the lower value of the scale is set to 10^{-3} s^{-1}) distribution during inlet phase: bullet initial velocity of 850 m/s, spin of 78.5 rad/s and impact angle respect to the shaft of 45 °C (right)

improvement in computing performances. With this aim the calibration of comprehensive material behavior is a key task in order to obtain reliable simulations.

Ballistic impact implies that the target material is subjected to very high strain rate combined with high levels of deformation, temperature and, of course, damage, especially in the zone very near to the impact. The great advantage on validated numerical approach is that a numerical model, able to reproduce correctly the damage due to an impact, could be used as base layer for evaluating the residual integrity of the impacted components in a wide variety of cases [1,2].

According to this objective, in a previous work [3], the Johnson-Cook model parameters were calibrated. In more details, the strain hardening coefficients (*A, B* and *n*) were numerically identified by comparison with a series of experimental tests on simple specimens, with similar geometry, but subjected to different stress triaxiality, thanks to the use of a multiaxial hydraulic test machine. On the other hand the strain rate hardening were obtained from literature and the temperature influence was not taken into account. The final goal was the numerical simulation of a component from helicopter tail rotor transmission, impacted by a bullet (Figure 1). In [1,2] the numerical model of the shaft (a tube) impacted by a projectile was modeled with the constitutive relation of Johnson-Cook (J-C) using parameters from [3]. In Figure 1 strain rate behaviour during bullet inlet phase is shown. A localized area reaches strain rate value that exceedes 10^3 s^{-1}; a very localized zone arrives to level of 10^6 s^{-1}.The main objective of this work is the improvement in the Al 6061 T6 alloy characterization starting from compression experimental data in order to obtain more suitable material model parameters to use in numerical simulations of complex structure subjected to ballistic impacts focusing the attention on the strain rate sensitivity.

2. Experimental tests

In this work the material Al 6061 T6 is experimentally characterized over a range of strain rates from 10^{-4} s^{-1} up to 10^4 s^{-1} in compression. Quasi-static loading condition is obtained via general purpose hydraulic testing machine, medium strain-rates tests are performed with pneumatic equipments and high strain rates tests are carried out with a Hopkinson pressure bar (Figure 2).

Figure 2 shows the experimental stress-strain rate behaviour for the material in comparison with the data obtained in [5]. Each set of data represents the difference between the stress values (e.g. evaluated in a certain range of plastic strain) and the stress value obtained in the lowest strain rate test.

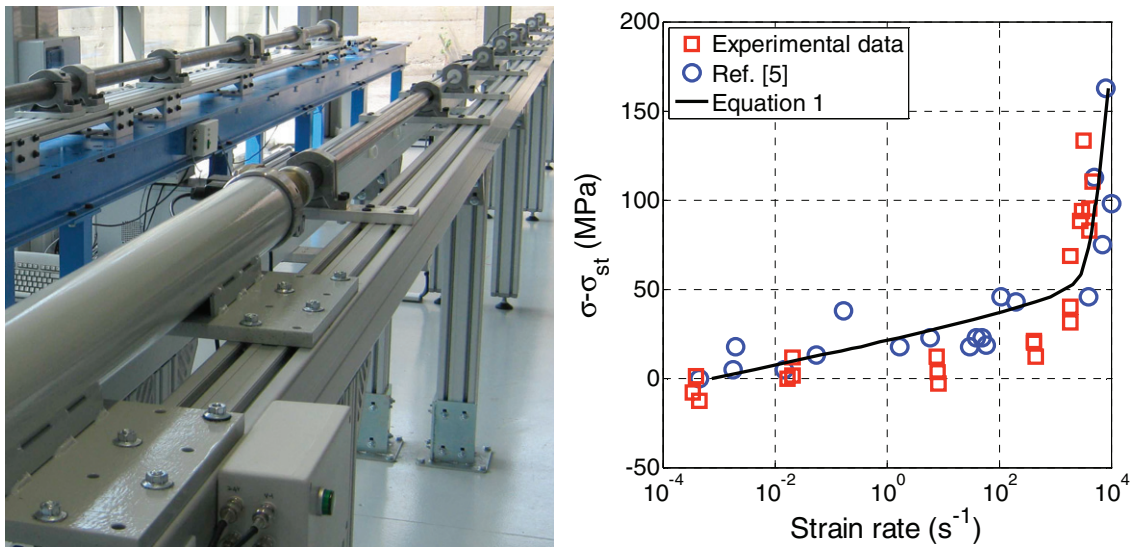

Fig. 2. Hopkinson Pressure Bar setup (left); stress-strain rate behavior in the semi-log plane (right): each set of data represents the difference between the stress values and the stress value obtained in the lowest strain rate test

The results obtained in this work are in trend with the data obtained from [5] and in both cases it is quite evident the dispersion of the experimental results. Besides, it is possible to conclude that until ~10^3 s^{-1} there is not a significant influence of the strain rate on the flow stress: all the experimental points are in a range of about 25 MPa. Over 10^3 s^{-1} of strain rate a change in the material behaviour is appreciable: the flow stress values are in a range of about 100 MPa. Another important consideration is that this type of diagram is incomplete since it does not take into account the temperature influence on the flow stress. At low strain rates (up to 10^2 s^{-1}) the deformation process can be considered isotherm, so the temperature influence can be neglected and the diagram of Figure 2 provides a sensible view of the material condition. On the other hand, a high strain rate phenomenon is strongly thermo-structural coupled: the structural-mechanics material conditions produce the rise in temperature that consequently modifies the mechanical material response. Usually, due to the rise in temperature, there is a decrease of the mechanical strength but also a modification (reduction) in the effect of the strain rate on the flow stress. Thermal softening phenomena are essentially due to heat conversion of mechanical work occurring at high strain rates where strain is localized. In general, starting from 10^2 s^{-1} of strain rate thermal diffusion (conduction and convection) can be neglected and thermal softening can be evaluated under adiabatic assumption. This implies the diagram of Figure 2 is partially inaccurate in this range of strain rate.

3. Strain rate sensitivity

The significant increase in the material strength over strain rate of 10^3 s^{-1} is usually identified by a change in the dislocation motion mechanism. At low strain rates the deformation rate is thermally activated: local obstacles and the Peierls stress barrier control the glide resistance. Dislocations are assumed to be pinned against barriers until a thermal fluctuation can kick them over the obstacle to glide to the next barrier. Instead, at high strain rate the glide kinetics should be entirely controlled by viscous phonon and electron drag.

In order to represent the complete rate deformation behavior detected for the Al 6061 T6 alloy it is needed a model such that proposed by [6] in which the plastic strain rate is correlated to the thermal stress component σ_T according with the relation

$$\dot{\varepsilon}_{pl} = \left(\frac{1}{C_1} \exp\left[\frac{2U_K}{k_b T} \left(1 - \frac{\sigma_T}{\sigma_P} \right)^2 \right] + \frac{C_2}{\sigma_T} \right)^{-1} \quad (1)$$

in which the first term expresses the thermal activated controlled glide and it is valid only if the $\sigma_T < \sigma_P$ that represents the Peierls stress and the second term expresses the linear relation between the thermal stress component and the strain rate in the phonon drag regime. In more details, the parameters C_1, C_2 and U_k are phenomenological and depends on the mobile dislocation density, the Burgers vector, the average distance between barriers and the scattering of lattice phonons. It is important to note that in this model the strain rate sensitivity is function of the temperature (thermal stress model) but only in the thermal activated part, while phonon drag is temperature indipendent. Using this type of model it is possible to fit the data dispersion of Figure 2 and the model approximation is in good agreement with the experimental data.

Since the experimental data distribution in the stress-strain rate plane can well approximate with a bilinear function and with the aim to simplify the strength material model to use in the numerical simulations, the Johnson-Cook material model is applied. The J-C model [4] is one of the most simple models able to predict the mechanical behaviour of the materials under different loading conditions. Besides, it is one of the most used material models, so it is implemented in many FEM codes and it is quite easy to find in literature the values of J-C parameters for different materials. In the J-C model only the athermal stress component is taken into account (the viscous effect is not directly influenced by the temperature) and the flow stress is expressed as

$$\sigma_y = \left(A + B\varepsilon_{\mathrm{pl}}^n \right) \left(1 + C \ln \frac{\dot{\varepsilon}_{\mathrm{pl}}}{\dot{\varepsilon}_0} \right) \left(1 - T^{*m} \right) \quad (2)$$

in which A is the elastic limit strength, B and n are the work hardening parameters, C and $\dot{\varepsilon}_0$ are the strain rate sensitivity coefficients and T^* and m describe the thermal softening.

4. Numerical parameters identification

In order to obtain the J-C material model parameters a numerical optimization is used. Aim of the inverse method is the determination of selected set of unknown parameters in a numerical model in order to correctly reproduce experimental tests with FEM calculations. In particular, in this work, the comparison is done in terms of force-displacement curves. Core of this procedure consists of iteratively solve numerical simulations (with the FEM code LS-DYNA [7]) having the experimental curves as objective functions. Optimization of the parameters is performed with dedicated algorithm included in the software LS-OPT [8]. The optimization algorithm works with a multiple objective function, this requires to run simultaneously all the simulations relative to a specific set of parameters that must be optimized.

Since J-C model is a multiplicative model it is possible to optimize separately each set of parameters. So, a first optimization is done in order to extract the strain dependence (A, B and n of the Equation 2). The second step requires the evaluation of the thermal softening parameters (m and T^* of the Equation 2) that are obtained from literature [5], and finally, the last optimization is done to extract the strain rate coefficients (C and $\dot{\varepsilon}_0$ of the Equation 2) from the dynamic tests.

In the first step, the starting (trial) points for the strain hardening coefficients optimization are the results obtained in [3] on the basis of different stress triaxiality tests (A=270 MPa, B=154.3 MPa and n=0.2215). Here, the optimization is done on the basis of the experimental results until 1 s^{-1} (Figure 3): the parameter A is fixed to 270 MPa and the optimized values are B=138.2 MPa and n=0.1792.

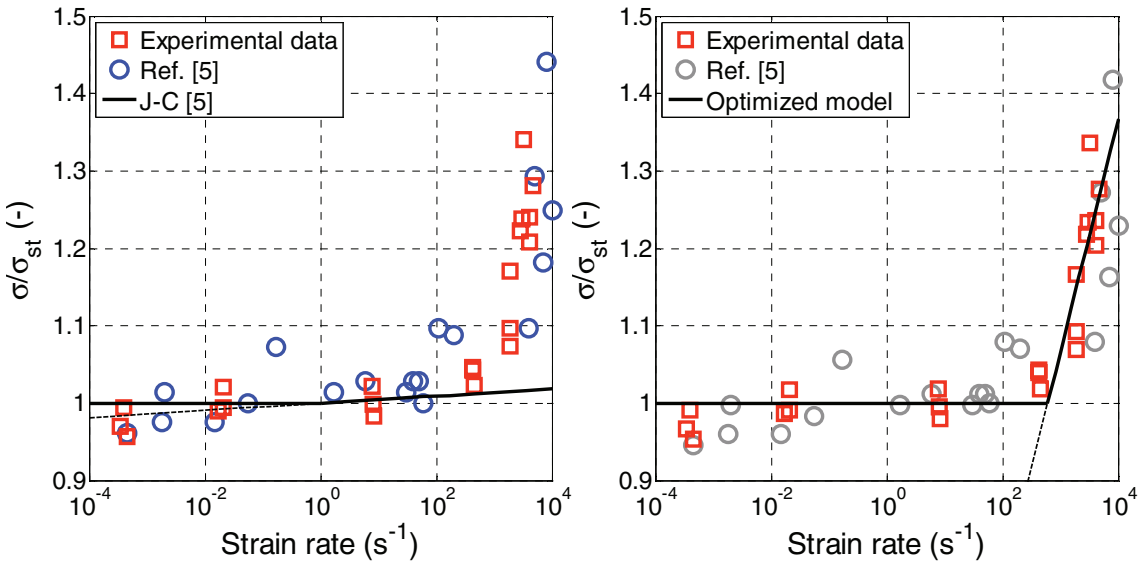

Fig. 3. Stress-strain rate behavior in the semi-log plane: C=0.002 and $\dot{\varepsilon}_0$ =1 s^{-1} (left); stress-strain rate behavior in the semi-log plane: C=0.1301 and $\dot{\varepsilon}_0$ =597.2 s^{-1} (right). In both cases the solid line is saturated at the value of 1 because in LS-DYNA $\dot{\varepsilon}_0$ represents the threshold under which the strain rate effects are negligible (the second term of the equation 2 is equal to the unity).

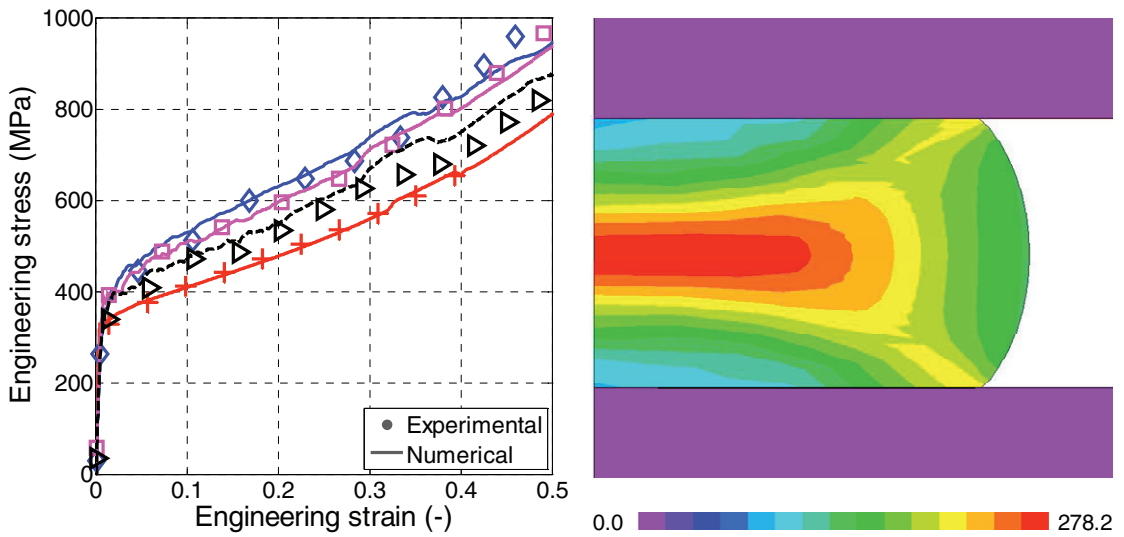

Fig. 4. Comparison between experimental end numerical stress-strain curves (up to 50% of deformation): ◇ ~4600 s^{-1}, □ ~3000 s^{-1}, ▷ ~1900 s^{-1}, + static (left); temperature increment distribution (K) in the specimen at ~4100 s^{-1} and 5 mm of stroke.

For what concerns the strain rate sensitivity identification, usually, only the parameter C is considered as an optimization variable, while $\dot{\varepsilon}_0$ is set equal to 1 s^{-1}. In Figure 3 there is the comparison between the experimental stress-strain rate results and the J-C model obtained with the strain rate sensitivity coefficients taken from [5]. The experimental data are shifted according to the requirement of $\dot{\varepsilon}_0$=1 s^{-1} and normalized respect to the stress obtained in the test at the lowest strain rate.

Since the final objective is the material model parameters identification in order to simulate ballistic impact scenario, it might be more sensible to focus the numerical inverse method on the basis of the high strain rate experimental tests (squared point over 10^2 s^{-1}), neglecting any strain rate effects at lower strain rates. In this case the optimized values are C=0.1301 and $\dot{\varepsilon}_0$=597.2 s^{-1} (Figure 3). It is important to remark that in Figure 3 the J-C line represents the material strenght model obtained via the numerical inverse optimization

In Figure 4 there is the comparison between the experimental and numerical optimized results in terms of stress-strain curves at different strain rates: the numerical results are in good agreement with the experimental data. The temperature distribution in the specimen is not uniform and it is proportional to the plastic strain distribution. In Figure 4 the temperature distribution calculated at 5 mm of stroke for the test at ~4100 s^{-1} is reported: the maximum temperature increase is about 280 K correspondent to a thermal softening scale factor of about 0.8.

5. Conclusion

In this work a combined experimental and numerical technique, based on an inverse approach, for material model identification was applied to the Al 6061 T6 alloy. The attention was focused on the strain rate sensitivity identification since the material finds several applications in ballistic impact scenario.

Experimental data dispersion was observed and compared with other results in literature. From the experimental data it was possible to conclude that until ~10^3 s^{-1} there is not a significant influence of the strain rate on the flow stress while over ~10^3 s^{-1} there is an appreciable increase in the strain rate sensitivity. Consequently, the strain rate dependence was supposed to be well approximated with a bilinear function and the material model strenght used was the Johnson-Cook model. The model parameters were obtained on the basis of the experimental tests performed in the strain rate range between 10^{-4} and 10^4 s^{-1}.

References

[1] L. Giudici, A. Manes, M. Giglio "Ballistic Impact on a Tail Rotor Transmission Shaft for Helicopter", Int Conf Ballistic 2010, May 17-21, 2010, Beijing, (China).

[2] A. Manes, M. Giglio, G. Magrassi, M. Bordegoni, “Reverse engineering of experimental tests results of ballistic impact for the validation of Finite Element Simulations”, Proceedings of the ASME 2010 International Design Engineering Technical Conferences & Computers and Information in Engineering Conference, IDETC/CIE 2010 , August 15-18, 2010, Montreal.

[3] A. Gilioli, A. Manes, M. Giglio, “Calibration of a constitutive material model for AL-6061-T6 aluminum alloy”, Proceeding of the ACE X, July 8-9, 2010, Paris, (France).

[4] G. R. Johnson, W. H. Cook “Fracture characteristics of three metals subjected to various strains, strain rates, temperatures and pressures”, Engineering Fracture Mechanics, 21, pp. 31–48 (1985)

[5] D. R. Leuser, G. J. Kay, M. M. LeBlanc, “Modeling Large-Strain, High-Rate Deformation in Metals”, 3th Biennial Tri-Lab. Eng. Conf. Modeling and Simulation, Nov. 3-5, 1999, Pleasaton (CA)

[6] D. J. Steinberg, C. M. Lund, “A constitutive model for strain rates from 10^{-4} to 10^6 s^{-1}”, Journal de physique, Symposium C3, (1988) 49:433-440

[7] Gladman, B., et al., LS-DYNA® Keyword User’s Manual – Vol. I – Version 971. LSTC (2007)

[8] N. Stander, et al. (2009) “LS-OPT® User’s manual – A Design Optimization And Probabilistic Analysis Tool For The Engineering Analysist”, Version 4.0, LSTC